IMA Journal of Applied Mathematics (1997) **59**, 1–23

Scattering of fluid loaded elastic plate waves at the vertex of a wedge of arbitrary angle, I: analytic solution

J. B. LAWRIE

Department of Mathematics and Statistics, Brunel University, Uxbridge, Middlesex UB8 3PH, *UK*

AND

I. D. ABRAHAMS

Department of Mathematics, Keele University, Keele, Staffs ST5 5BG, *UK*

[Received 27 June 1996]

This article is the first part of an investigation into the scattering of fluid coupled structural waves by an angular discontinuity at the junction of two plates of different material properties. These two thin elastic plates are semi-infinite in extent therefore forming the faces of an infinite wedge, the interior of which contains a compressible fluid. A plane unattenuated structural wave is incident along the lower face of the wedge and is scattered at the apex. The edges of the elastic plates may be joined in a variety of different ways, for example, they may be pin-jointed to an external structure or welded to each other. In the former case, the plates will experience only the usual flexural vibrations whereas in the latter case longitudinal (in-plane) disturbances will be generated and will propagate away from the wedge apex.

An exact explicit solution is sought in terms of a Sommerfeld integral representation for the fluid velocity potential. This permits the boundary-value problem to be recast as a functional difference equation which is easily solved in terms of the Maliuzhinets special function (Maliuzhinets, *Soviet Phys. Dokl.* **3** 1958). The chosen ansatz for the solution is of a different form from that used previously by the authors for the less complicated membrane wedge problem. The new ansatz has several analytic and numerical advantages which enable the reflection and transmission coefficients to be expressed explicitly in a compact form that is ideal for computation.

In the second part of this study a full numerical investigation of the reflection and transmission coefficients will be presented for a variety of interesting parameter ranges and edge conditions.

1. Introduction

The transmission and reflection of waves at discontinuities in physical structures has long been of interest to engineers. Examples include electromagnetic and acoustical waveguides, where the material properties of the propagating medium, the cross-sectional area of the guide, or the properties of the boundary itself, may all change abruptly. Such effects are utilized in vehicle silencer design to 'smooth out' the pressure fluctuations created by the engine and hence reduce the noise emission. The same problems can arise in solid structures, where vibrational waves created by engines, gearboxes, external turbulent flows or other hydroelastic sources often propagate with little loss of energy. At abrupt changes in the

structure those elastic (or other) waves may reflect or scatter some of this energy, sometimes with quite large and deleterious effects. Submarines are mainly composed of structural members covered by thin metal plates or shells, both of which are good waveguides for transmitting the engine's low-frequency vibrations. At, for example, points where the elastic plates are welded together or whenever side-spars are connected to the main members this energy can be channelled and indeed focused. It is not uncommon for parts of such structures that are quite remote from the vibrational source to have quite serious noise problems.

To understand the way in which energy is distributed around a complex structure it is necessary to study the fundamental component problems: the weld point; the point where one member joins another etc. These individual scatterers cannot easily be combined to obtain the full solution, as multiple reflections or scattering often occurs, but their solution is required none the less. This paper will concentrate on the transmission problem for elastic waves on thin plates in underwater or aeroacoustic situations. It is a straightforward matter to calculate the *in vacuo* transmission and reflection of elastic waves at the interface of two planar, semi-infinite flat plates, of different materials, joined at their edges. However, the same is not true if one or both sides of the plates are immersed in fluid since the structural wave energy can be shed into the fluid via complex scattering at plate edges. This important problem was first studied by Brazier-Smith (1987) and again recently by Norris and Wickham (1995). In both papers the Wiener–Hopf technique was employed. In a similar vein Cannell (1975) solved the problem of diffraction of plane acoustic waves in an infinite fluid containing a semi-infinite plate. It is not only discontinuities in material properties that cause reflection and scattering of plate waves, a change in slope can have the same effect. The fundamental problem for investigation in this context is that of two semi-infinite thin elastic plates, joined at their free edges and containing within the wedge thus formed a compressible fluid. For ease of mathematical exposition fluid is only contained in the interior wedge region, $-\beta < \theta < \beta$, where θ and β are illustrated in Fig. 1.

The model problem is perhaps most physically interesting because there are a wide variety of ways in which the two plate edges can be joined. These can lead to very different reflection, transmission and scattering results, including the mode conversion from flexural to longitudinal vibrations. For example, the two plates can be clamped to an external structure so that their displacements and slopes at the edge are zero. Alternatively, if there are no external forces or moments at the wedge apex, and the plates are hinged, then each plate experiences a force from the other plate, but zero moment. In the former case no in-plane, or longitudinal, vibrations are induced whereas the latter example will generate such travelling waves. For multiple scattering problems, involving several 'inner' problems of this type, it is important to understand and classify all these possible cases and to calculate the energy at infinity in each component. The induced longitudinal motions from one apex may travel a long distance with little attenuation (these are not coupled to the fluid) but then scatter energy into the fluid and structure when next it meets an angular discontinuity. This paper therefore seeks to

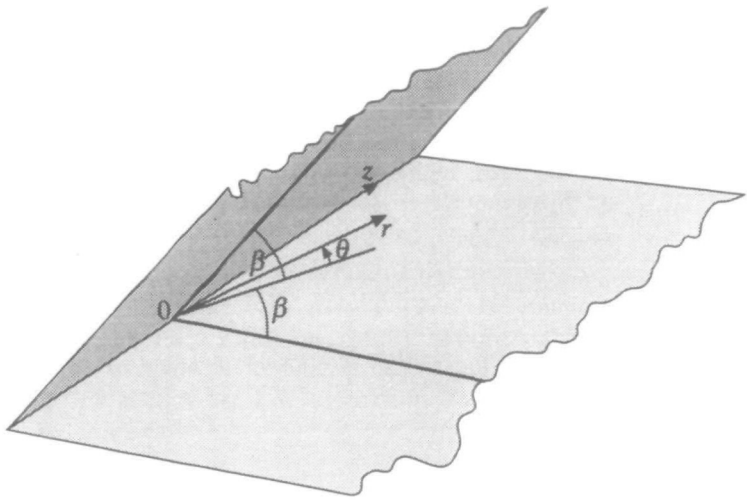

FIG. 1. The physical configuration

present a solution to the plate/fluid wedge model for general edge conditions and plate types. An exact, explicit solution is presented in a form convenient for numerical evaluation, and a complete classification of all the edge conditions is made. In order not to overface the reader, the work is split into two parts. This, the first article, is concerned with a brief derivation of the exact solution for arbitrary plate and fluid parameter values and wedge angle. The reflection and transmission coefficients for unattenuated plate waves are explicitly given herein, as well as a prescription of the procedure for the complete range of edge conditions. In part II, numerical results will be presented for a variety of physically interesting cases.

The solution method of this work employs a Sommerfeld integral representation. This is the natural far-field form for a function which is most easily expressed in polar coordinates and which satisfies the wave equation. For boundary-value problems in which the wedge faces are of impedance or higher-order type (that is, consisting of combinations of the unknown function and its derivatives normal and tangential to the surface), then the application of a Sommerfeld transform reduces the problem to a functional difference equation. Maliuzhinets (1958) and Williams (1959) were the first to solve such equations for impedance boundaries. For higher-order conditions, such a membrane or elastic plate, Maliuzhinets's approach does not follow through in a straightforward manner. Instead, particular solutions of the difference equation must be added in correct combinations to ensure satisfaction of the specific edge conditions. This was suggested by Osipov (1994) and independently by Abrahams and Lawrie (1995) and Lawrie and Abrahams (1996), the latter articles addressing the fluid loaded membrane wedge for *arbitrary* wedge angle. Recently, Osipov and Norris (Osipov & Norris, 1996; Norris & Osipov, 1996) have also turned their attention to plane wave scattering by membrane and elastic faced wedges.

This article builds upon the work presented in (Abrahams & Lawrie, 1995) and so for brevity the solution scheme is merely offered to the reader rather than derived. A more extensive bibliography can be found in that paper. However, it is worth mentioning here that an alternative approach to the solution of such problems was offered by Abrahams (1986, 1987) who then employed the Kontorovich–Lebedev transform, which is the analogue of the Mellin transform for the wave equation. Further alternative procedures for wedge-type scattering problems (for example, see (Davis, 1996)) are available in the literature, but these are not so useful for high-order boundary conditions.

There is a significant increase in complexity of the solution when comparing the present boundary-value problem for two arbitrary elastic plates with that of the membrane wedge. This is due to the additional number of edge constraints required, the number of attenuated coupled plate wave modes and the potential coupling to in-plane plate vibrations. In order to simplify the analytical form of the solution, and to significantly reduce the associated difficulties of computing the particular integrals, it is most convenient here to work with a solution ansatz modified from that offered in (Abrahams & Lawrie, 1995). It can be shown (Lawrie & Abrahams, 1996) that the two are in fact equivalent to each other (as they must be since the solution is unique), and to that proposed by Norris and Osipov (1996). This point will be amplified in the text.

The paper is organized as follows. In the following section the boundary-value problem is reduced, via the introduction of a Sommerfeld integral representation, to a pair of coupled inhomogeneous difference equations satisfied by a function with certain specified analyticity properties. This function is assumed to a take a special form (3.4) in Section 3.1, which is shown to satisfy the difference equations. A precise number of free coefficients in this solution are to be specified by satisfaction of the plate edge conditions. By expanding the solution about the apex in Section 3.2, these coefficients are related directly to the plate displacements and their derivatives at the edges. In this way a low-order linear system of equations for these coefficients is obtained, which can be inverted for any given set of edge constraints. Having fully specified the solution, Section 4 yields the reflection and transmission plate wave coefficients due to an incoming unattenuated plate wave. These will be evaluated in part II for a range of interesting edge conditions and across all wedge angles. The comprehensive range of such conditions, and their mathematical specifications, is the subject of the penultimate Section, 5. Finally, concluding remarks to this article are presented in Section 6.

2. The boundary-value problem

An inviscid compressible fluid, of sound speed c_0 and density ρ, occupies the wedge shaped region defined in terms of a cylindrical polar coordinate system (r, θ, z) by $-\beta < \theta < \beta$, $0 \leqslant r < \infty$. The fluid is bounded by two thin elastic plates which, when undisturbed, lie along the rays $\theta = \pm\beta$. A small disturbance to either plate or to the fluid will result in a fluid pressure perturbation, $p(r, \theta, z, t)$, which satisfies the usual wave equation. The fluid pressure and plate motions,

$\eta^{\pm}(r, z, t)$ (where the superscripts + and − are used to denote the displacements of the upper and lower plates respectively), are coupled through the fluid velocity potential, $\Phi(r, \theta, z, t)$, according to the relationships

$$p(r, \theta, z, t) = -\rho \frac{\partial \Phi}{\partial t}(r, \theta, z, t) \tag{2.1}$$

and

$$\frac{\partial \eta^{\pm}}{\partial t}(r, z, t) = \frac{1}{r}\frac{\partial \Phi}{\partial \theta}(r, \pm\beta, z, t). \tag{2.2}$$

In this article it is assumed without loss of generality that the small disturbance takes the form of a plane structural wave of unit amplitude and raidan frequency ω which propagates from infinity along the lower plate towards the wedge apex. The incident wave is incorporated into the fluid velocity potential and has the form

$$\Phi^{i}(r, \theta, z, t) = \mathrm{Re}\{e^{-ikr\cos(X_1-\beta-\theta)}e^{-i\omega t}\} \tag{2.3}$$

where the constant X_1 is defined later in the text and $k = \omega/c_0$ is the fluid wavenumber. This choice of forcing together with the physical geometry ensures that the scattered sound field is independent of z. A solution with harmonic time dependence is sought and using this information the two dimensional velocity potential may be expressed in the form

$$\Phi(r, \theta, t) = \mathrm{Re}\{\phi(r, \theta)e^{-i\omega t}\}. \tag{2.4}$$

For convenience the time dependence is henceforth suppressed.

The full boundary-value problem can now be stated in terms of the complex velocity potential, $\phi(r, \theta)$, as

$$\left\{\frac{\partial^2}{\partial r^2} + \frac{1}{r}\frac{\partial}{\partial r} + \frac{1}{r^2}\frac{\partial^2}{\partial \theta^2} + k^2\right\}\phi(r, \theta) = 0 \tag{2.5}$$

with 'plate' boundary conditions given by

$$\left\{\frac{\partial^4}{\partial r^4} - \mu^4\right\}\frac{1}{r}\frac{\partial \phi}{\partial \theta} + \alpha_1\phi = \sum_{n=1}^{4} A_n(-ik)^{5-n}\delta^{(n-1)}(r), \qquad \theta = -\beta \tag{2.6}$$

and

$$\left\{\frac{\partial^4}{\partial r^4} - \nu^4\right\}\frac{1}{r}\frac{\partial \phi}{\partial \theta} - \alpha_2\phi = \sum_{n=1}^{4} B_n(-ik)^{5-n}\delta^{(n-1)}(r), \qquad \theta = +\beta. \tag{2.7}$$

In (2.6), (2.7) the quantity μ (ν) is the *in vacuo* wavenumber and α_1 (α_2) is the fluid loading parameter for the lower (upper) plate (for definitions of these quantities see, for example, (Cannell, 1975)). The terms on the right-hand side of (2.6) and (2.7) are a linear combination of the Dirac delta function and its derivatives. These correspond directly to physical forces and moments applied to the plates at the wedge apex (Leppington, 1978). A discussion of these quantities

is given in Section 5; however, it is important to note here that the full specification of the boundary-value problem requires appropriate edge conditions to be applied to both plates at $r = 0$. The edge conditions depend on the physical problem under consideration and it is not uncommon for different conditions to be applied to the lower and upper plates. The coefficients A_n and B_n in (2.6) and (2.7) are defined such that they have the same physical dimensions as the fluid velocity potential; the factor $(-ik)^{5-n}$ is introduced purely for algebraic convenience in the subsequent analysis. Finally, in addition to (2.5), (2.6) and (2.7) it is necessary to impose certain restrictions on the velocity potential. That is, $\phi(r, \theta)$ must be finite at $r = 0$ and, with the exception of the incident wave (2.3) and its images, must comprise only of outgoing or decaying waves as $r \to \infty$.

In order to obtain an exact solution of the above boundary-value problem it is convenient to express the velocity potential as a Sommerfeld integral. Thus,

$$\phi(r, \theta) = \frac{1}{2\pi i} \int_{\gamma} f(s + \theta) e^{-ikr\cos(s)} \, ds, \tag{2.8}$$

where the path of integration comprises a $\cup$-shaped loop lying above the real axis and a $\cap$-shaped loop lying below the real axis; see Fig. 2. Any singularities

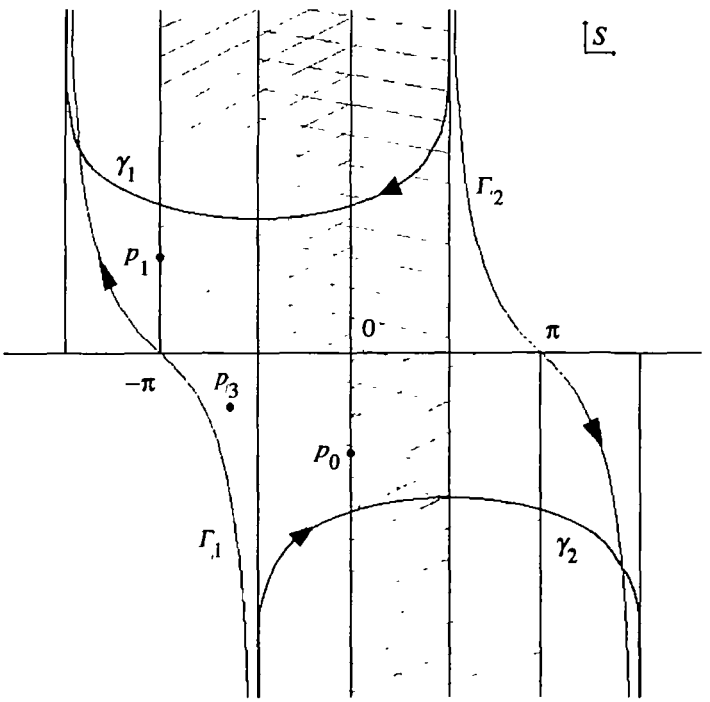

FIG. 2. The complex s-plane showing the Sommerfeld integration contour $\gamma = \gamma_1 + \gamma_2$. Any poles lying in the right-hatched region (that is, hatching with negative slope) correspond to incoming waves, and poles in the left-hatched region (positive slope lines) give exponentially growing terms as $r \to \infty$. Also, Γ_1 and Γ_2 are the steepest descent contours, and the poles at p_j, $j = 0, 1, 3$ correspond to the unattenuated incoming wave, an unattenuated outgoing wave, and a typical leaky wave respectively

of the integrand (which only take the form of poles) lie strictly outside the regions enclosed by either loop; those of physical interest are contained between the horizontal portions of both loops. Note that the upper loop commences at $\pi/2 + i\infty$, loops round the hill of the exponent at a finite point of the complex s-plane, and terminates at $-3\pi/2 + i\infty$. Similarly, the lower loop starts at $-\pi/2 - i\infty$ and ends at $3\pi/2 - i\infty$. It is easy to deduce that, expressed in this form, the velocity potential automatically satisfies the reduced wave equation. The object is thus to determine the function $f(s + \theta)$ such that $\phi(r, \theta)$ satisfies (2.6), (2.7). An additional requirement on $f(s + \theta)$ is that, with the exception of the poles corresponding to the incident wave and appropriate images, its poles must lie in the correct regions of the complex s-plane to represent only outgoing waves. On substituting (2.8) into (2.6) and (2.7) and using the properties of the Sommerfeld integral to represent each delta function in the appropriate form (see (Abrahams & Lawrie, 1995)), it is found that $f(s)$ satisfies the following two functional difference equations:

$$P(s)f(s-\beta) + \bar{P}(s)f(-s-\beta) = -\sum_{n=1}^{4} A_n \cos^{n-1}(s)\sin(s), \tag{2.9}$$

$$\bar{Q}(s)f(s+\beta) + Q(s)f(-s+\beta) = -\sum_{n=1}^{4} B_n \cos^{n-1}(s)\sin(s), \tag{2.10}$$

where

$$P(s) = \sin^5(s) - 2\sin^3(s) + a\sin(s) + ic, \quad \bar{P}(s) = -P(-s), \tag{2.11}$$

$$Q(s) = \sin^5(s) - 2\sin^3(s) + b\sin(s) + id, \quad \bar{Q}(s) = -Q(-s), \tag{2.12}$$

and the non-dimensional coefficients are defined by $a = 1 - \mu^4/k^4$, $c = \alpha_1/k^5$, $b = 1 - \nu^4/k^4$, $d = \alpha_2/k^5$. It is convenient to write $P(s)$, $Q(s)$ in the following form:

$$P(s) = \prod_{j=1}^{5} \sin(s) - \sin(X_j), \qquad Q(s) = \prod_{j=1}^{5} \sin(s) - \sin(Y_j), \tag{2.13}$$

where

$$\mathrm{Re}(X_1), \mathrm{Re}(Y_1) = 0, \qquad \mathrm{Im}(X_1), \mathrm{Im}(Y_1) < 0 \tag{2.14}$$

correspond to the wavenumbers of unattenuated plate waves on the lower and upper surfaces respectively (see 2.3). The other complex-valued coefficients are defined to lie in the ranges

$$-\pi/2 \leqslant \mathrm{Re}(X_3), \mathrm{Re}(Y_3) < 0, \qquad \mathrm{Im}(X_3), \mathrm{Im}(Y_3) > 0, \tag{2.15}$$

$$-\pi/2 \leqslant \mathrm{Re}(X_5), \mathrm{Re}(Y_5) < 0, \qquad \mathrm{Im}(X_5), \mathrm{Im}(Y_5) < 0, \tag{2.16}$$

and

$$X_j = -\bar{X}_{j+1}, \qquad Y_j = -\bar{Y}_{j+1}, \qquad j = 2, 4, \tag{2.17}$$

where the overbar in the last equation signifies complex conjugate.

3. Exact solution of the boundary-value problem

3.1 *Solution of the difference equations*

It is a relatively straightforward procedure to write down a suitable ansatz for the solution of the difference equations (2.9), (2.10). From a previous paper by the authors (Abrahams & Lawrie, 1995) the chosen ansatz could take the form

$$f(s) = f_0(s)\left\{\sigma(s+\beta, X_1) + \sum_{n=1}^{4} A_n g_n(s) + \sum_{n=1}^{4} B_n h_n(s)\right\}, \tag{3.1}$$

where $f_0(s)$ is a solution to the homogeneous system of difference equations, the functions $g_n(s)$, $h_n(s)$ are particular solutions of (2.9), (2.10) and $\sigma(s+\beta, X_1)$ is an eigensolution which corresponds to the incident surface wave on the lower plate together with its images. The precise form of this eigensolution is found by noting that an unattenuated plate wave on the lower wedge surface has wavenumber corresponding to X_1 and that the pole that gives rise to this wave term must lie in the region of the complex s-plane that corresponds to incoming waves. For convenience, the incident wave is chosen to have unit amplitude and thus, following Maliuzhinets (1958), $\sigma(s, z)$ is defined as

$$\sigma(s, z) = -\frac{\pi}{4\beta}\sin\frac{\pi z}{2\beta}\Big/\sin\frac{\pi}{4\beta}(z+s)\sin\frac{\pi}{4\beta}(z-s). \tag{3.2}$$

This eigensolution can be easily shown to satisfy the relations

$$\sigma(\alpha, z) = \sigma(-\alpha, z), \qquad \sigma(\alpha+2\beta, z) = \sigma(\alpha-2\beta, z). \tag{3.3}$$

The ansatz, given in expression (3.1), is not the only form of solution possible. Indeed, other forms may be more or less convenient for the purposes of this paper. Norris and Osipov (1996) postulated an alternative ansatz to (3.1), but the computationally most efficient form (as will be discussed later) is taken to be

$$f(s) = f_0(s)\sigma(s+\beta, X_1)\sigma(s-\beta, Y_1)\left\{\sum_{n=1}^{4} A_n g_n(s) + \sum_{n=1}^{4} B_n h_n(s)\right\}. \tag{3.4}$$

The eigensolution $\sigma(s-\beta, Y_1)$ includes an incoming wave contribution (and its images) on the upper plate which, by correct choice of the constants A_n, B_n, must be removed if no such forcing is insinuated.

The function $f_0(s)$ is defined for the general wedge problem in (Lawrie & Abrahams, 1996) and the appropriate form for this particular problem is

$$f_0(s) = f_1(s)f_2(s), \tag{3.5}$$

$$f_1(s) = \prod_{j=1}^{5} M_\beta\left(s - X_j - \beta + \frac{\pi}{2}\right)M_\beta\left(s + X_j - \beta - \frac{\pi}{2}\right), \tag{3.6}$$

$$f_2(s) = \prod_{j=1}^{5} M_\beta\left(s - Y_j + \beta + \frac{\pi}{2}\right)M_\beta\left(s + Y_j + \beta - \frac{\pi}{2}\right), \tag{3.7}$$

where the reflection relations $f_1(s+\beta)=f_1(\beta-s)$ and $f_2(s-\beta)=f_2(-s-\beta)$ should be noted. The Maliuzhinets function, $M_\beta(z)$, was first defined in a paper by Maliuzhinets (1958) and its properties are given in some detail in (Abrahams & Lawrie, 1995, Appendix A). It remains to define the particular solutions $g_n(s), h_n(s)$. These sets of functions ($n=1,2,3,4$) are particular integrals of the difference equations (2.9) and (2.10). Each set of functions is defined in terms of a pair of constant-coefficient first-order functional difference equations which are obtained by substituting $\sigma(s+\beta, X_1)\sigma(s-\beta, Y_1)f_0(s)g_n(s)$ and $\sigma(s+\beta, X_1)\sigma(s-\beta, Y_1)f_0(s)h_n(s)$ into (2.9) and (2.10) respectively. Thus, using (3.3), $g_n(s)$ satisfies

$$g_n(s)-g_n(s+4\beta)=-\frac{\cos^{n-1}(s+\beta)\sin(s+\beta)}{f_0(s)P(s+\beta)\sigma(s+\beta, X_1)\sigma(s-\beta, Y_1)} \tag{3.8}$$

and

$$g_n(s+\beta)=g_n(\beta-s), \tag{3.9}$$

whilst $h_n(s)$ satisfies

$$h_n(s)-h_n(s-4\beta)=-\frac{\cos^{n-1}(s-\beta)\sin(s-\beta)}{f_0(s)\bar{Q}(s-\beta)\sigma(s+\beta, X_1)\sigma(s-\beta, Y_1)}, \tag{3.10}$$

$$h_n(s-\beta)=h_n(-s-\beta). \tag{3.11}$$

It is a relatively straightforward procedure to obtain integral representations for $g_n(s)$ and $h_n(s)$ as defined by (3.8) to (3.11). Full details of the method by which these are derived are given in (Abrahams & Lawrie, 1995); a similar representation, for general inhomogeneous terms is given by Tuzhilin (1973). For brevity we merely quote the appropriate results to be

$$g_n(s)=\frac{-\mathrm{i}}{8\beta\cos\{(\pi(s+\beta)/4\beta\}}$$
$$\times\int_{-\mathrm{i}\infty}^{\mathrm{i}\infty}\frac{\cos^{n-1}(\alpha)\sin(\alpha)\cos(\pi\alpha/4\beta)}{P(\alpha)f_0(\alpha-\beta)\sigma(\alpha, X_1)\sigma(\alpha-2\beta, Y_1)\sin\{(\pi(\alpha-\beta-s)/4\beta\}}d\alpha, \tag{3.12}$$

and

$$h_n(s)=\frac{\mathrm{i}}{8\beta\cos\{(\pi(s-\beta)/4\beta\}}$$
$$\times\int_{-\mathrm{i}\infty}^{\mathrm{i}\infty}\frac{\cos^{n-1}(\alpha)\sin(\alpha)\cos(\pi\alpha/4\beta)}{\bar{Q}(\alpha)f_0(\alpha+\beta)\sigma(\alpha+2\beta, X_1)\sigma(\alpha, Y_1)\sin\{\pi(\alpha+\beta-s)/4\beta\}}d\alpha. \tag{3.13}$$

The integral representation for $g_n(s)$ is defined for s lying in the strip $0<\mathrm{Re}\,(s+\beta)<4\beta$ indented around several of the zeros of $P(\alpha)f_0(\alpha)$ as shown in Fig. 3. The bounding line of the strip at 4β is of identical form to that shown (that is, the strip is the area swept out by moving the contour in Fig. 3 a distance 4β to the right). Note that the indentations shown in Fig. 3 at $\pm(Y_j+2\beta)$, $j=3,5$

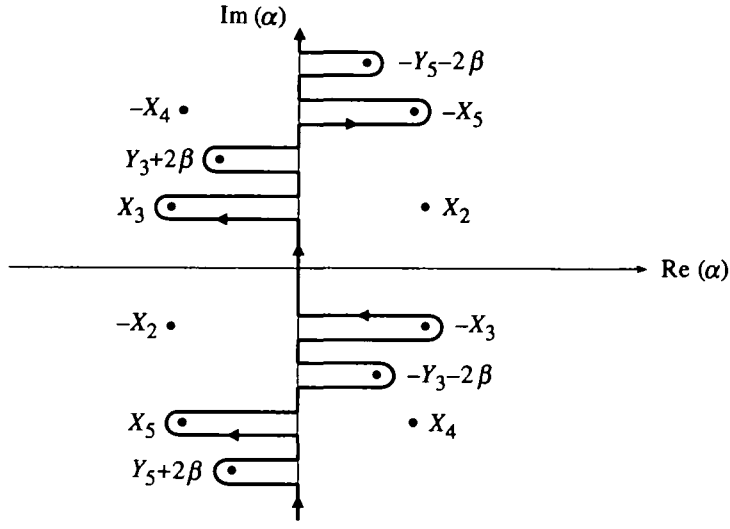

FIG. 3. Integration contour for $g_n(s)$ indented around the pole singularities of the integrands

only occur for small enough wedge angles: $\beta < -\mathrm{Re}\,(Y_j)/2$, $j = 3, 5$. For values of s outside this strip it is necessary to employ the difference equation (3.8) as a continuation formula. Likewise, the integral representation for $h_n(s)$ is defined for s lying in $-4\beta < \mathrm{Re}\,(s-\beta) < 0$, again suitably indented. This is the strip formed by taking the contour shown in Fig. 3, interchanging the X and Y labels, and then moving this contour a distance 4β to the left. Thus, for $h_n(s)$, $-Y_3$ lies within the strip, but not $X_3 + 2\beta$ etc. For values of s outside the strip, (3.10) is the continuation formula of $h_n(s)$.

3.2 *The near-field expansion*

Embedded in expression (3.4) are the constants A_n and B_n, $n = 0, 1, 2, 3$ which, as yet, have not been specified. At least eight conditions (depending on the edge constraints and incoming wave specification, see Section 5) are required in order to determine these constants. Two independent conditions are obtained by insisting that $f(s)$ is $O(1)$ as $s \to \pm\infty$. The latter constraint is necessary in order that the fluid velocity potential be bounded as $r \to 0$. It is a straightforward procedure to show that

$$f_0(s) = O(\mathrm{e}^{-5\mathrm{i}\pi s/2\beta}), \qquad s \to \mathrm{i}\infty, \tag{3.14}$$

and

$$\sigma(s, X) = -\frac{\pi}{\beta}\sum_{j=1}^{\infty} \sin(j\pi X/2\beta)\mathrm{e}^{\pm \mathrm{i}j\pi s/2\beta}, \qquad \mathrm{Im}\,(s) \gtrless \pm|\mathrm{Im}\,(X)|. \tag{3.15}$$

It follows that the terms in the parentheses of (3.4) must be $O(\mathrm{e}^{3\mathrm{i}\pi s/2\beta})$ as $s \to \mathrm{i}\infty$. In order to enforce this behaviour it is necessary to determine the behaviour of

$g_n(s)$ and $h_n(s)$ as $s \to i\infty$. Fortunately, the asymptotic forms for the quantities $g_n(s)$ and $h_n(s)$ are easily derived and are quoted here as

$$g_n(s) = \sum_{j=1}^{2} \kappa_{jn} e^{j\pi s/2\beta} + O(e^{3j\pi s/2\beta}), \qquad s \to i\infty, \tag{3.16}$$

$$h_n(s) = \sum_{j=1}^{2} \lambda_{jn} e^{j\pi s/2\beta} + O(e^{3j\pi s/2\beta}), \qquad s \to i\infty, \tag{3.17}$$

where the coefficients κ_{jn} and λ_{jn}, $n = 1, \ldots, 4$, $j = 1, 2$ are given in explicit integral form by

$$\kappa_{jn} = \frac{i(-1)^{j+1}}{2\beta} \int_{-i\infty}^{i\infty} \frac{\cos^{n-1}(\alpha) \sin(\alpha) \sin\{j\pi(\alpha + 2\beta)/4\beta\} e^{-j\pi\alpha/4\beta}}{P(\alpha) f_0(\alpha - \beta) \sigma(\alpha, X_1) \sigma(\alpha - 2\beta, Y_1)} \, d\alpha \tag{3.18}$$

and

$$\lambda_{jn} = \frac{-i(-1)^{j+1}}{2\beta} \int_{-i\infty}^{i\infty} \frac{\cos^{n-1}(\alpha) \sin(\alpha) \sin\{j\pi(\alpha + 2\beta)/4\beta\} e^{-j\pi\alpha/4\beta}}{\tilde{Q}(\alpha) f_0(\alpha + \beta) \sigma(\alpha, Y_1) \sigma(\alpha - 2\beta, X_1)} \, d\alpha. \tag{3.19}$$

Enforcement of the correct growth at infinity, that is, eliminating the $e^{j\pi s/2\beta}$ and $e^{j\pi s/\beta}$ terms within the parentheses of (3.4), gives two equations for the unknown edge coefficients. Thus,

$$\sum_{n=1}^{4} A_n \kappa_{jn} + \sum_{n=1}^{4} B_n \lambda_{jn} = 0, \qquad j = 1, 2. \tag{3.20}$$

As already mentioned, the ansatz (3.4) will, as written, give incoming unattenuated transverse plate waves on both upper and lower plates. These arise from poles at $s = X_1 - \beta$, $-Y_1 + \beta$ in the explicit σ terms, $\sigma(s + \beta, X_1)$, $\sigma(s - \beta, Y_1)$ respectively. To eliminate the incoming upper plate wave, its residue is set to zero:

$$\sum_{n=1}^{4} A_n g_n(-Y_1 + \beta) + \sum_{n=1}^{4} B_n h_n(-Y_1 + \beta) = 0 \tag{3.21}$$

and to enforce the lower incoming plate wave amplitude to be unity, the residue of $f(s)$ at $X_1 - \beta$ must be 1:

$$f_0(X_1 - \beta) \sigma(X_1 - 2\beta, Y_1) \left(\sum_{n=1}^{4} A_n g_n(X_1 - \beta) + \sum_{n=1}^{4} B_n h_n(X_1 - \beta) \right) = 1. \tag{3.22}$$

For convenience, the constants in (3.21) and (3.22) are written as

$$g_n(-Y_1 + \beta) = \kappa_{3n}, \qquad h_n(-Y_1 + \beta) = \lambda_{3n}, \tag{3.23}$$

$$g_n(X_1 - \beta) = \kappa_{4n}, \qquad h_n(X_1 - \beta) = \lambda_{4n}, \tag{3.24}$$

for all n, so that the four equations may be written as

$$\mathbf{K}\mathbf{A} + \Lambda\mathbf{B} = \mathbf{F}, \tag{3.25}$$

where the elements of $\mathbf{K}, \Lambda$ are $\kappa_{jn}, \lambda_{jn}, j, n = 1, 2, 3, 4$ respectively, whilst the vectors $\mathbf{A}$, $\mathbf{B}$ and $\mathbf{F}$ are comprised of A_n, B_n and

$$\mathbf{F} = \frac{1}{f_0(X_1 - \beta)\sigma(X_1 - 2\beta, Y_1)} \begin{pmatrix} 0 \\ 0 \\ 0 \\ 1 \end{pmatrix}. \tag{3.26}$$

This matrix system is incomplete, viz. four equations for eight unknowns, and further equations for A_n and B_n must be added before these constants are fully determined. These additional conditions are obtained by applying the edge conditions, and in order for this to be done it is necessary to obtain the near-field expansion of the plate displacements.

The near-field behaviour of the plates, that is, the form of $\eta^{\pm}(r)$ as $r \to 0$, is found by rewriting the integral expression for $\eta^{\pm}(r)$ as

$$\eta^{\pm}(r) = \frac{-ik}{2\pi\omega} \int_{\gamma_1} \sin(s)\{f(s \pm \beta) + f(-s \pm \beta)\} e^{-ikr\cos(s)}\, ds, \tag{3.27}$$

where the path of integration is the upper of the two loops which together comprise γ (see Fig. 2). Consider the plate lying along the ray $\theta = -\beta$; the behaviour of $\eta^{-}(r)$ as $r \to 0$ is obtained by expanding the integrand as $|s| \to \infty$ and then integrating term by term. (As explained in (Abrahams & Lawrie, 1995), this process is permissible because there are no poles within the loop γ_1 and thus it can be moved upwards as far from the origin as desired.) It is a straightforward matter to show that

$$\sin(s)\{f(s-\beta) + f(-s-\beta)\} = -8ie^{3is}\{1 - 5e^{2is}\} \sum_{n=1}^{4} A_n \cos^{n-1}(s) + O(e^{4is}), \quad s \to i\infty. \tag{3.28}$$

On substituting this expression into (3.27) and utilizing the result

$$-\frac{1}{2\pi} \int_{\gamma_1} e^{i\nu s} e^{-ikr\cos(s)}\, ds = J_\nu(kr) e^{-i\nu\pi/2} \tag{3.29}$$

it is found that

$$ic_0\eta^{-}(r) \sim 8 \sum_{n=1}^{4} \frac{A_n}{(-ik)^{n-1}} \frac{\partial^{n-1}}{\partial r^{n-1}} \{J_3(kr) + 5J_5(kr)\}, \quad r \to 0, \tag{3.30}$$

where c_0 is the fluid sound speed. It is now easily deduced that

$$c_0\eta^{-}(r) \sim A_4 + A_3(-ikr) + A_2\frac{(-ikr)^2}{2!} + A_1\frac{(-ikr)^3}{3!}, \quad r \to 0 \tag{3.31}$$

and a similar analysis for the upper plate yields the result

$$c_0\eta^+(r) \sim B_4 + B_3(-ikr) + B_2\frac{(-ikr)^2}{2!} + B_1\frac{(-ikr)^3}{3!}, \quad r \to 0. \tag{3.32}$$

These two expansions will be employed in Section 5 to deduce the remaining coefficient equations for a range of different edge conditions.

4. The reflection and transmission coefficients

Of considerable interest in any application of the model problem are the reflection and transmission coefficients and it is instructive to be able to plot these quantities as a function of the wedge half-angle β. In order to do so uniform expressions must be obtained and this section deals with the derivation of these formulae.

The reflection coefficient is the residue contribution to $\phi(r, \theta)$ arising from the pole at $s = -X_1 - \pi - \beta$. That is, using R to denote the reflection coefficient,

$$R = \lim_{s \to -X_1 - \pi - \beta} (s + X_1 + \pi + \beta) f_0(s)\sigma(s + \beta, X_1)\sigma(s - \beta, Y_1) \times \left\{ \sum_{n=1}^{4} A_n g_n(s) + \sum_{n=1}^{4} B_n h_n(s) \right\}. \tag{4.1}$$

This pole lies to the left of the strip $-\beta < \mathrm{Re}\,(s) < 3\beta$ for which the integral representation for $g_n(s)$ is defined. However, for $\mathrm{Re}\,(s) < -\beta$ a valid expression for $g_n(s)$ is easily obtained by recourse to the difference equation (3.8). This gives an expression in terms of $g_n(s + 4j\beta)$, where the counter j is chosen such that $s + 4j\beta$ lies in the indented strip. In order that the final expression for R be both uniform in β and easily computable, it is expedient to re-express $g_n(s + 4j\beta)$ in terms of an integral whose path of integration is *straight* along the imaginary axis from 0 to $+i\infty$. This is achieved by first contracting the range of integration of (3.12) onto the upper portion of the contour and then subtracting out various poles. The final expression for $g_n(s)$, $\mathrm{Re}\,(s) < -\beta$ comprises of a sum of j terms arising from application of the difference equation together with a straight line integral, $g_n^*(s + 4j\beta)$ and four finite sums of residues. A similar procedure is demonstrated in greater detail in (Lawrie & Abrahams, 1996). Thus, for $\mathrm{Re}\,(s) < -\beta$, it is found that

$$g_n(s) = g_n^*(s + 4j\beta) - \frac{G_n(s + \beta, j)}{\sigma(s + \beta, X_1)\sigma(s - \beta, Y_1)f_0(s)P(s + \beta)} - \sum_r \frac{\tilde{Q}(r - 2\beta)\sigma(s + \beta, r)G_n(r, p_r)}{[Q(s - 2\beta)P(s)]'\,|_{s=r}\, f_0(-r + 3\beta)\sigma(r, X_1)\sigma(r - 2\beta, Y_1)}, \tag{4.2}$$

where $[\,]'\,|_{s=r}$ indicates the derivative of the quantity in square brackets evaluated at $s = r$, r takes the four values

$$r = X_3, \quad X_5, \quad Y_3 + 2\beta, \quad Y_5 + 2\beta, \tag{4.3}$$

p_r is the associated integer such that

$$-\frac{\mathrm{Re}\,(r)}{4\beta} < p_r < -\frac{\mathrm{Re}\,(r)}{4\beta} + 1 \tag{4.4}$$

and j has the integer value

$$-\frac{1}{4} - \frac{\mathrm{Re}\,(s)}{4\beta} < j < \frac{3}{4} - \frac{\mathrm{Re}\,(s)}{4\beta}. \tag{4.5}$$

Further, $g_n^*(z)$ is the straight line integral

$$g_n^*(z) = \frac{\mathrm{i}}{2\pi}\int_0^{\mathrm{i}\infty} \frac{\cos^{n-1}(\alpha)\sin(\alpha)\sigma(z+\beta,\alpha)}{P(\alpha)f_0(\alpha-\beta)\sigma(\alpha,X_1)\sigma(\alpha-2\beta,Y_1)}\,\mathrm{d}\alpha, \tag{4.6}$$

in which $-\beta < z < 3\beta$, and

$$G_n(z,p) = \sum_{m=0}^{p-1} \cos^{n-1}(z+4m\beta)\sin(z+4m\beta) \times \prod_{\ell=1}^{m} \frac{\bar{P}(z+4(\ell-1)\beta)\bar{Q}(z-2\beta+4\ell\beta)}{P(z+4\ell\beta)Q(z-2\beta+4\ell\beta)}. \tag{4.7}$$

Note that $G_n(z,p) = 0$ if $p \leqslant 0$, which corresponds to the situation in which no poles are traversed during deformation to a vertical contour. Also, in (4.7) and below, the product $\prod_{\ell=1}^{0}$ is taken as unity.

Likewise, the point $s = -X_1 - \pi - \beta$ lies in or to the left of the strip $-3\beta < \mathrm{Re}\,(s) < \beta$ and it follows that a similar procedure must be employed in order to obtain valid and computable forms for the functions $h_n(s)$. In this case the counter u is chosen such that $-3\beta < s + 4u\beta < \beta$ and it is found that

$$h_n(s) = h_n^*(s+4u\beta) + \frac{\bar{P}(t-2\beta)H_n(s+3\beta,u)}{\sigma(s+\beta,X_1)\sigma(s-\beta,Y_1)f_0(s)P(s+\beta)Q(s+3\beta)} - \sum_t \frac{\sigma(s-\beta,t)\bar{P}(t-2\beta)H_n(t,q_t)}{[P(s-2\beta)Q(s)]'\,|_{s=t} f_0(t-3\beta)\sigma(t+2\beta,X_1)\sigma(t,Y_1)}, \tag{4.8}$$

in which

$$-\frac{\mathrm{Re}\,(t)}{4\beta} < q_t < -\frac{\mathrm{Re}\,(t)}{4\beta} + 1 \tag{4.9}$$

for each of the values of t

$$t = Y_3, \quad Y_5, \quad X_3 + 2\beta, \quad X_5 + 2\beta, \tag{4.10}$$

and

$$-\frac{3}{4} - \frac{\mathrm{Re}\,(s)}{4\beta} < u < \frac{1}{4} - \frac{\mathrm{Re}\,(s)}{4\beta}. \tag{4.11}$$

Also

$$h_n^*(z) = \frac{-\mathrm{i}}{2\pi}\int_0^{\mathrm{i}\infty} \frac{\cos^{n-1}(\alpha)\sin(\alpha)\sigma(z-\beta,\alpha)}{\bar{Q}(\alpha)f_0(\alpha+\beta)\sigma(\alpha+2\beta,X_1)\sigma(\alpha,Y_1)}\,\mathrm{d}\alpha, \tag{4.12}$$

where again the path of integration is straight, $-3\beta < \mathrm{Re}\,(z) < \beta$, and

$$H_n(z,q) = \sum_{m=0}^{q-1} \cos^{n-1}(z+4m\beta)\sin(z+4m\beta) \times \prod_{\ell=1}^{m} \frac{\tilde{P}(z-2\beta+4\ell\beta)\tilde{Q}(z+4(\ell-1)\beta)}{P(z-2\beta+4\ell\beta)Q(z+4\ell\beta)} \tag{4.13}$$

for $q > 0$. In a similar fashion to $G_n(z,p)$, the term $H_n(z,q) = 0$ for $q \leqslant 0$.

Using $g_n(s)$ and $h_n(s)$ in the forms given above it is now possible to evaluate expression (4.1). Note that in the second terms of (4.2), (4.8) the pole at $s = -X_1 - \pi - \beta$ comes from a zero of the polynomial $P(s+\beta)$ in the denominator and not from $f_0(s)$ as this function is cancelled. After some effort it is found that

$$\begin{aligned} R = &-\frac{4\beta}{\pi}\sin\frac{\pi^2}{4\beta}\sigma(X_1+\pi,X_1)\sigma(X_1+\pi+2\beta,Y_1)M_\beta(2\beta-\pi/2)M_\beta(2X_1+2\beta+\pi/2) \\ &\times \prod_{\ell=2}^{5} M_\beta(X_1+X_\ell+2\beta+\pi/2)M_\beta(X_1-X_\ell+2\beta+3\pi/2) \\ &\times \prod_{\ell=1}^{5} M_\beta(X_1+Y_\ell+\pi/2)M_\beta(X_1-Y_\ell+3\pi/2) \\ &\times \sum_{n=1}^{4}\Big\{A_n g_n^*(-X_1-\pi-\beta+4j\beta)+B_n h_n^*(-X_1-\pi-\beta+4u\beta) \\ &- A_n \sum_r \frac{\tilde{Q}(r-2\beta)\sigma(X_1+\pi,r)G_n(r,p_r)}{[Q(s-2\beta)P(s)]'\,|_{s=r}\, f_0(3\beta-r)\sigma(r,X_1)\sigma(r-2\beta,Y_1)} \\ &- B_n \sum_t \frac{\tilde{P}(t-2\beta)\sigma(X_1+\pi+2\beta,t)H_n(t,q_t)}{[P(s-2\beta)Q(s)]'\,|_{s=t}\, f_0(t-3\beta)\sigma(t+2\beta,X_1)\sigma(t,Y_1)}\Big\} \\ &+ \sum_{n=1}^{4}\frac{A_n G_n(-X_1-\pi,j)}{P'(X_1)} - \sum_{n=1}^{4}\frac{B_n H_n(-X_1-\pi+2\beta,u)\tilde{P}(X_1)}{P'(X_1)Q(X_1-2\beta)}. \end{aligned} \tag{4.14}$$

In contrast to that for the reflection coefficient, the pole that gives rise to the transmission coefficient lies to the right of the indented strip $-3\beta < \mathrm{Re}\,(s) < \beta$ at the point $s = Y_1 + \pi + \beta$. This has little effect on the analysis other than that the difference equations for $g_n(s)$ and $h_n(s)$ must be iterated in the opposite direction. Using T to denote the transmission coefficient it is found that

$$T = \lim_{s\to Y_1+\pi+\beta}(s-Y_1-\pi-\beta)f_0(s)\sigma(s+\beta,X_1)\sigma(s-\beta,Y_1) \times \Big\{\sum_{n=1}^{4} A_n g_n(s) + \sum_{n=1}^{4} B_n h_n(s)\Big\}. \tag{4.15}$$

After a considerable amount of algebra this can be expressed in the form

$$T = \frac{4\beta}{\pi}\sin\frac{\pi^2}{4\beta}\sigma(Y_1+2\beta+\pi, X_1)\sigma(Y_1+\pi, Y_1)M_\beta(2\beta-\pi/2)M_\beta(2Y_1+2\beta+\pi/2)$$

$$\times\prod_{\ell=2}^{5} M_\beta(Y_1+Y_\ell+2\beta+\pi/2)M_\beta(Y_1-Y_\ell+2\beta+3\pi/2)$$

$$\times\prod_{\ell=1}^{5} M_\beta(Y_1+X_\ell+\pi/2)M_\beta(Y_1-X_\ell+3\pi/2)$$

$$\times\sum_{n=1}^{4}\Big\{A_n g_n^*(Y_1+\beta+\pi-4u\beta)+B_n h_n^*(Y_1+\beta+\pi-4j\beta)$$

$$-A_n\sum_r \frac{\tilde{Q}(r-2\beta)\sigma(Y_1+2\beta+\pi, r)G_n(r, p_r)}{[Q(s-2\beta)P(s)]'\big|_{s=r} f_0(3\beta-r)\sigma(r, X_1)\sigma(r-2\beta, Y_1)}$$

$$-B_n\sum_t \frac{\tilde{P}(t-2\beta)\sigma(Y_1+\pi, t)H_n(t, q_t)}{[P(s-2\beta)Q(s)]'\big|_{s=t} f_0(t-3\beta)\sigma(t+2\beta, X_1)\sigma(t, Y_1)}\Big\}$$

$$+\sum_{n=1}^{4}\frac{A_n\tilde{Q}(Y_1)G_n(2\beta-Y_1-\pi, u)}{P(Y_1-2\beta)Q'(Y_1)}-\sum_{n=1}^{4}\frac{B_n H_n(-Y_1-\pi, j)}{Q'(Y_1)}. \tag{4.16}$$

5. The edge conditions

In the previous section it was noted that only four conditions for the constants A_n and B_n, $n = 1, 2, 3, 4$ can be specified by imposing finiteness of fluid pressure and the correct incoming wave condition. Therefore, four additional conditions are required and these are obtained by consideration of the physical constraints applied to the plates at the wedge apex. However, for certain important cases six conditions are in fact required because of the necessary introduction of two extra scalar constants. In these rather special situations the matrix system (which incorporates (3.25)) is thus increased in size to 10×10.

In this section a variety of edge conditions will be described. The first subsection deals with the simplest sets of edge conditions corresponding to situations in which the plate edges do not interact. For example, the plate displacements may be zero and the gradients or moments specified. In these cases, all possible combinations of uncoupled constraints lead to four additional conditions for the coefficients A_n, B_n. The second subsection deals with the more complicated situation which can arise when the wedge apex is free to rotate and translate in space (that is, no external forces constrain the apex displacement). The edge conditions on both plates are now intrinsicially coupled and this results in the generation of 'in-plane' as well as 'out-of-plane' displacements within the plate. Such motions are incorporated into the analysis of the edge behaviour and, as mentioned above, this increases the size of the system of linear equations to be solved.

5.1 *Independent edge conditions*

The simplest edge conditions are those that may be applied to the two plates independently. These are appropriate if the wedge apex is constrained by external forces or moments in such a way as to fix its location in space, or if the plate edges move without touching. Below are summarized the most commonly found constraints acting on thin plates, and note should be taken of the fact that either plate can independently experience any one of them.

(I) *Clamped plate.* A clamped edge, often referred to as 'built-in', constrains the plate to maintain zero displacement and gradient. That is,

$$\eta(0) = \eta_r(0) = 0, \tag{5.1}$$

which, if applied to the upper surface, gives

$$B_4 = B_3 = 0 \tag{5.2}$$

from (3.32), and when specified to the lower plate gives, from (3.31),

$$A_4 = A_3 = 0. \tag{5.3}$$

(II) *Pin-jointed.* Either plate may be pin-jointed to a fixed point in space, in which case it will be constrained to have zero displacement and zero moment at the origin. It is easy to show that this yields the edge-conditions

$$\eta(0) = \eta_{rr}(0) = 0, \tag{5.4}$$

which translates to the coefficient values

$$B_4 = B_2 = 0 \tag{5.5}$$

when applied to the upper plate, and

$$A_4 = A_2 = 0 \tag{5.6}$$

for the lower surface.

(III) *Free edge.* A third set of conditions is appropriate to the common situation in which the edge of a plate is free of both external moments and forces. In terms of the plate displacement (Junger & Feit, 1986):

$$\eta_{rr}(0) = \eta_{rrr}(0) = 0 \tag{5.7}$$

and so, from (3.32),

$$B_2 = B_1 = 0 \tag{5.8}$$

for a free upper plate, and

$$A_2 = A_1 = 0 \tag{5.9}$$

for the same condition applied to the lower one. Note, these only hold if the two plates do not touch each other during their motion.

In some physical situations it may be appropriate, as mentioned above, to apply different edge conditions to the two plates. For example, the lower plate may be

free (III) whilst the upper plates is clamped (I) which corresponds to the conditions

$$A_2 = A_1 = B_4 = B_3 = 0. \tag{5.10}$$

Alternatively, the lower plate may be pin-jointed (II) whilst the upper plate is free (III) which gives rise to conditions (5.6) and (5.8). Any combination of the clamped, pin-jointed or free edge conditions may be applied to the plates although, obviously, some sets of conditions are more realistic than others.

Certain physical situations can arise in which the edges are partially constrained. That is, external forces may restrict the motion of the apex to one direction only. For example a sliding pin-joint permits motion in a specified direction (say, vertically or horizontally). Partially constrained edges will generate in-plane compressional waves of the type discussed fully in the next subsection.

5.2 *Coupled edge*

If the wedge apex is free to move in space then in general the edge constraints applied to the two plates will be coupled. As a thin elastic plate resists motion in both its transverse and longitudinal directions, it is also necessary to account for in-plane motion. That is, compressional waves of the type that couple to transverse vibrations in shells and shell-like structures (see, for example, (Lawrie, 1986) or (Zhang & Abrahams, 1995). In-plane plate motion is usually governed by a linearized wave equation of the form

$$\frac{\partial^2 \zeta^{\pm}}{\partial r^2} + (k_p^{\pm})^2 \zeta^{\pm} = 0, \tag{5.11}$$

where $\zeta^{\pm}$ is the in-plane displacement in the upper (lower) plate, $k_p^{\pm} = \omega / c_p^{\pm}$,

$$(c_p^{\pm})^2 = \frac{E^{\pm}}{\rho_p^{\pm}(1 - (\nu^{\pm})^2)} \tag{5.12}$$

is the square of the speed of compressional waves in the upper (lower) plate, and $E^{\pm}$, $\rho_p^{\pm}$, $\nu^{\pm}$ are the Young's modulus, density and Poisson's ratio of the respective surfaces. Note that the plate coefficients μ and ν appearing in (2.6), (2.7) are related to the compressional wavenumber via

$$\nu^2 = \sqrt{12}\, k_p^{+}/h^{+}, \qquad \mu^2 = \sqrt{12}\, k_p^{-}/h^{-} \tag{5.13}$$

in which $h^{\pm}$ is the thickness of the corresponding plate.

On taking the outgoing solution of (5.11) and expanding for small r, it is found that

$$\begin{aligned} \zeta^{\pm}(r) &= \zeta_0^{\pm} e^{ik_p^{\pm} r} \\ &\sim \zeta_0^{\pm}\left\{1 + ik_p^{\pm} r - \frac{(k_p^{\pm})^2}{2!} r^2 + \cdots\right\}, \quad r \to 0, \end{aligned} \tag{5.14}$$

where $\zeta_0^{\pm}$ are the transmission coefficients of the in-plane waves. These two unknowns must be determined along with the coefficients A_n and B_n of (3.4), and so two additional conditions are required on top of the four already discussed in Section 5.1.

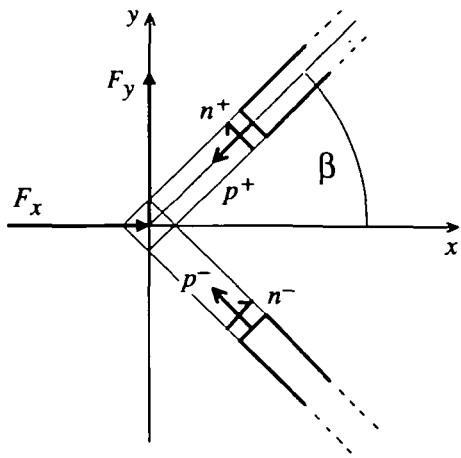

FIG. 4. The external force applied at the plate edges (F_x, F_y) and the normal and shear stresses in the upper and lower plates

Before examining specific cases, it is useful to obtain general edge conditions for coupled plates. First, any external forces at the wedge vertex must be balanced, for all time, by stresses in the plates. Figure 4 illustrates this balance, where $\mathrm{Re}\,(F_x e^{-i\omega t})$, $\mathrm{Re}\,(F_y e^{-i\omega t})$ are external forces (per unit span in the z-direction) applied in the horizontal and vertical directions respectively, and $p^\pm$ and $n^\pm$ are the longitudinal (normal) and transverse (shear) stresses generated by the upper and lower plates as shown. Resolving forces gives

$$(h^+p^+ + h^-p^-)\cos\beta + (h^+n^+ - h^-n^-)\sin\beta = F_x, \tag{5.15}$$

$$(h^+p^+ - h^-p^-)\sin\beta - (h^+n^+ + h^-n^-)\cos\beta = F_y. \tag{5.16}$$

The stresses at the elastic plate edges are easily related to the unknown coefficients (Junger & Feit, 1986), and are found to be

$$h^\pm p^\pm = d^\pm \zeta_0^\pm, \quad h^+n^+ = c^+B_1, \quad h^-n^- = c^-A_1, \tag{5.17}$$

where

$$d^\pm = i\omega h^\pm \rho_p^\pm c_p^\pm, \qquad c^\pm = -i\frac{(\omega h^\pm)^3 \rho_p^\pm}{12 c_p^\pm c_0}. \tag{5.18}$$

Second, the condition that the plates remain in contact at the wedge apex gives, by resolving displacements, the following relationship between the two plate edges:

$$\begin{pmatrix} \zeta_0^- \\ A_4/c_0 \end{pmatrix} = \begin{pmatrix} \cos(2\beta) & -\sin(2\beta) \\ \sin(2\beta) & \cos(2\beta) \end{pmatrix} \begin{pmatrix} \zeta_0^+ \\ B_4/c_0 \end{pmatrix}. \tag{5.19}$$

Here, B_4/c_0, A_4/c_0 are the transverse displacements at the origin of the upper and lower plates respectively, as is easily seen from (3.31), (3.32).

(IV) *Hinged corner.* The case of two plates joined by at their edges by a frictionless hinge is now examined. If there is no external support to hold the

edge in place then there are no forces, $F_x = F_y = 0$, and the hinge implies that both plates experience zero torque. The latter condition gives, as in (II) above (5.4), (5.5),

$$A_2 = B_2 = 0 \tag{5.20}$$

and with zero forces:

$$(d^+\zeta_0^+ + d^-\zeta_0^-)\cos\beta + (c^+B_1 - c^-A_1)\sin\beta = 0, \tag{5.21}$$

$$(d^+\zeta_0^+ - d^-\zeta_0^-)\sin\beta - (c^+B_1 + c^-A_1)\cos\beta = 0. \tag{5.22}$$

Hence (5.20) to (5.22) and continuity at the edge (5.19) give six equations. These, with (3.25), give ten equations for the ten unknowns $A_n, B_n, n = 1, \ldots, 4$ and $\zeta_0^\pm$ and so all the coefficients can be determined.

(V) *Welded corner.* If the two plates are welded together, and not constrained by external forces or moments, then the apex angle can be (approximately) assumed to remain fixed at 2β. Therefore, the constant angle condition

$$\eta_r^+(0) = \eta_r^-(0) \tag{5.23}$$

and zero external moment

$$\eta_{rr}^+(0) + \eta_{rr}^-(0) = 0 \tag{5.24}$$

replace the edge conditions (5.20) above. Hence, in terms of the unknown coefficients,

$$B_3 = A_3, \qquad B_2 = -A_2, \tag{5.25}$$

equations (5.21), (5.22), (5.19) and (3.25) specify the problem uniquely.

(VI) *Sliding pin-joint.* As an example of more complicated edge conditions, the case of a pin-joint, free to slide in the horizontal direction only, will be considered. If the joint is assumed to be frictionless then it is a hybrid of conditions (II) and (IV) above. First, displacements are in the horizontal direction only, and so, from continuity (5.19),

$$\zeta_0^+\cos\beta - (B_4/c_0)\sin\beta = \zeta_0^-\cos\beta + (A_4/c_0)\sin\beta, \tag{5.26}$$

$$\zeta_0^+\sin\beta + (B_4/c_0)\cos\beta = -\zeta_0^-\sin\beta + (A_4/c_0)\cos\beta = 0. \tag{5.27}$$

Secondly, no moment on each plate edge allows (5.20) to hold and finally, zero force in the horizontal direction implies (5.21). Once again, (5.26), (5.27), (5.20) and (5.21) give six equations, which with (3.25) are enough to determine all the ten unknown coefficients. Most other edge conditions which may be encountered can be dealt with in an identical fashion.

6. Discussion and conclusions

In this article an ansatz for the solution to scattering of fluid coupled structural waves at an angular discontinuity has been presented. That ansatz has been applied to determine the reflected and transmitted waves generated when a plane structural wave is incident towards the apex of a fluid wedge of arbitrary

angle bounded by two elastic plates of dissimilar material properties. As mentioned previously, the solution is different in form from those offered by Abrahams and Lawrie (1995) and Osipov and Norris (1996) for the solution of the membrane wedge problem. The new ansatz, whilst undoubtedly equivalent to these previous formulations, has several advantages which make it both particularly compact in form and useful for computational purposes. To recapitalate, the function $f(s)$ is assumed to take the form

$$f(s) = f_0(s)\sigma(s+\beta, X_1)\sigma(s-\beta, Y_1)\Big\{\sum_{n=1}^{4} A_n g_n(s) + \sum_{n=1}^{4} B_n h_n(s)\Big\}, \qquad (6.1)$$

where the quantities $f_0(s)$, $\sigma(s, z)$, $g_n(s)$ and $h_n(s)$ are defined in equations (3.5) to (3.11). The eigensolutions $\sigma(s+\beta, X_1)$, $\sigma(s-\beta, Y_1)$ contain poles at $X_1-\beta$, $-Y_1+\beta$ which correspond to incoming structural waves on the lower and upper plates respectively. Thus, there is a choice of forcing and without loss of generality one pole can be suppressed by suitable choice of the constants A_n and B_n. In this article the forcing was introduced along the lower plate.

One advantage of this form of the solution is that the particular integrals $g_n^*(s)$ and $h_n^*(s)$ ((4.6) and (4.12) respectively) assume a simpler form than those used previously, in that the integrand is free of poles *on* the path of integration. This avoids the need to remove such singularities by subtracting out appropriate terms from the integrand (Abrahams & Lawrie, 1995) or for a principal value interpretation of the integrals (Osipov & Norris, 1996). Numerically, this avoids a considerable amount of work in obtaining an accurate evaluation; for example, in the approach employed previously by the authors, the term subtracted in order to remove the singularity decayed (as $\alpha \to \mathrm{i}\infty$) with a different exponent to that of the original integrand.

Further, the ansatz used herein is symmetric with respect to forcing and geometry. One can choose whether to introduce the forcing term along the lower plate or the upper plate simply by swopping the right-hand sides of (3.21) and (3.22). This reflects the inherent symmetry in the problem; that is,

$$\phi(r, \theta) = \phi_a(r, -\theta), \qquad (6.2)$$

where ϕ_a is the adjoint wedge problem in which the upper and lower plates, and the incident plate forcing, are interchanged. A consequence of (6.2) is that, simply by interchanging X_j and Y_j, $j = 1, 2, 3, 4, 5$, the results for the adjoint problem can be retrieved directly from the solution presented here. Using $\hat{\ }$ to denote the operation of replacing X_j by Y_j, it is a simple matter to show that

$$\hat{P}(s) = Q(s), \quad \hat{A}_n = -B_n, \quad \hat{B}_n = -A_n \qquad (6.3)$$

and

$$\hat{f}_0(s) = f_0(-s), \quad \hat{g}_n^*(s) = h_n^*(-s), \quad \hat{h}_n^*(s) = g_n^*(-s). \qquad (6.4)$$

It follows that

$$\hat{R} = T_a, \qquad \hat{T} = R_a \qquad (6.5)$$

which indicates that the reflection and transmission coefficients for the adjoint problem (R_a and T_a) are obtained by interchanging X_j and Y_j in the transmission

and reflection coefficients obtained in Section 4. This provides a useful check on the solution, and can easily be verified for (4.14) and (4.16).

Finally, it should be noted that the forcing can be generalized. Instead of a structural wave, in fact any incident wave can be taken. The solution form then becomes, for example,

$$f(s) = f_0(s)\sigma(s+\beta, \theta_0+\beta)\sigma(s-\beta, Y_1)\Big\{\sum_{n=1}^{4} A_n g_n(s) + \sum_{n=1}^{4} B_n h_n(s)\Big\}, \quad (6.6)$$

where θ_0 is the (complex) angle of incidence of the plane wave forcing term and can take any value inside the strip $0 < \mathrm{Re}\,(\theta_0+\beta) < 2\beta$ indented as shown in Fig. 3. The symmetry of the solution is not lost but, with the generalized forcing given in (6.6), the particular integrals $g_n(s)$ now have contours indented around the singularities on the imaginary line at $\pm X_1$. Whilst considerably less convenient for computational purposes, this poses no insurmountable problem and may be dealt with as discussed above. Note that the particular integrals $h_n(s)$ do not exhibit the same problem.

To summarize, this article is the first part of an investigation into the scattering of structural waves at an angular discontinuity. Expressions for the reflection and transmission coefficients have been derived and a full discussion of the various edge conditions has been presented. In the second part of this work comprehensive numerical results will be offered for a range of edge conditions and across all wedge angles (that is, $0 < \beta < \pi$). Particular emphasis will be given to edge conditions and combinations of fluid and elastic plate constants that are of physical interest. Of particular focus will be the amount of the incident wave energy which is converted into each of the reflected and transmitted transverse and longitudinal plate modes and into the scattered field.

References

Abrahams, I. D., 1986 Diffraction by a semi-infinite membrane in the presence of a vertical barrier. *J. Sound Vib.* **111**, 191–207.

Abrahams, I. D., 1987 On the sound field generated by membrane surface waves on a wedge-shaped boundary. *Proc. R. Soc.* A **411**, 239–250.

Abrahams, I. D. & Lawrie, J. B., 1995 Travelling waves on a membrane: reflection and transmission at a corner of arbitrary angle, I. *Proc. R. Soc.* A **451**, 657–683.

Brazier-Smith, P. R., 1987 The acoustic properties of two co-planar half-planes plates. *Proc. R. Soc.* A **409**, 115–139.

Cannell, P. A., 1975 Edge scattering or aerodynamic sound by a lightly loaded elastic half-plane. *Proc. R. Soc.* A **347**, 213–238.

Davis, A. M. J., 1996 2-dimensional acoustical scattering by a penetrable wedge. *J. Acoust. Soc. Am.* **100**, 1316–1324.

Junger, M. C. & Feit, D., 1986 *Sound, Structures and their Interaction,* 2nd edition. Cambridge, USA: MIT Press.

Leppington, F. G., 1978 Acoustic scattering by membranes and plates with line constraints. *J. Sound Vib.* **58**, 319–332.

Lawrie, J. B., 1986 Vibrations of a heavily loaded semi-infinite cylindrical elastic shell. I. *Proc. R. Soc.* A **408**, 103–128.

Lawrie, J. B. & Abrahams, I. D., 1996 Travelling waves on a membrane: reflection and transmission at a corner of arbitrary angle, II. *Proc. R. Soc.* A **452**, 1649–1677.

MALIUZHINETS, G. D., 1958 Excitation, reflection and emission of surface waves from a wedge with given face impedances. *Soviet Phys. Dokl.* **3**, 752–755.

NORRIS, A. N. & OSIPOV, A. V., 1996 Structural and acoustical wave interaction at a wedge-shaped junction of fluid loaded plates. *J. Acoust. Soc. Am.* **101**, 867–876.

NORRIS, A. N. & WICKHAM, G. R., 1995 Acoustic diffraction from the junction of two flat plates. *Proc. R. Soc.* A **451**.

OSIPOV, A. V. & NORRIS, A. N., 1997 Sound diffraction by a sharp ridge on a fluid loaded membrane. *Proc. R. Soc.* A submitted.

OSIPOV, A. V., 1994 General solution for a class of diffraction problems. Letter to *J. Phys.* A: *Math. Gen.* **27**, L27–L32.

TUZHILIN, A. A., 1973 The theory of Malyuzhints' inhomogeneous functional equations. *Differentsial'nye Uravneniya* **9**, 2058–2064 (Russian translation available).

WILLIAMS, W. E., 1959 Diffraction of an E-polarized plane wave by an imperfectly conducting wedge. *Proc. R. Soc.* A **252**, 376–393.

ZHANG, B. & ABRAHAMS, I. D., 1995 The radiation of sound from a finite ring-forced cylindrical elastic shell. I: Wiener-Hopf analysis. *Proc. R. Soc.* A **450**, 89–108.